

Ultra-low permittivity ULTCC composite materials

Cite as: Appl. Phys. Lett. **118**, 142901 (2021); <https://doi.org/10.1063/5.0048566>

Submitted: 24 February 2021 . Accepted: 26 March 2021 . Published Online: 05 April 2021

 Mikko Nelo, Timo Vahera, Tuomo Siponkoski, Jari Juuti, and Heli Jantunen

COLLECTIONS

Paper published as part of the special topic on [Advances in 5G Physics, Materials, and Devices](#)



View Online



Export Citation



CrossMark

ARTICLES YOU MAY BE INTERESTED IN

[Theoretical and experimental study of shear mode bulk acoustic wave transformer based on c-axis zigzag ScAlN multilayer for rectenna application](#)

Applied Physics Letters **118**, 142903 (2021); <https://doi.org/10.1063/5.0041623>

[Perspective on ceramic materials for 5G wireless communication systems](#)

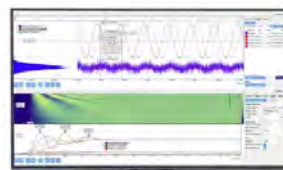
Applied Physics Letters **118**, 120501 (2021); <https://doi.org/10.1063/5.0036058>

[A hybrid optoelectronic Mott insulator](#)

Applied Physics Letters **118**, 141901 (2021); <https://doi.org/10.1063/5.0044066>

Challenge us.

What are your needs for periodic signal detection?



Zurich
Instruments



Ultra-low permittivity ULTCC composite materials

Cite as: Appl. Phys. Lett. **118**, 142901 (2021); doi: [10.1063/5.0048566](https://doi.org/10.1063/5.0048566)

Submitted: 24 February 2021 · Accepted: 26 March 2021 ·

Published Online: 5 April 2021



View Online



Export Citation



CrossMark

Mikko Nelo,^{a)}  Timo Vahera, Tuomo Siponkoski, Jari Juuti, and Heli Jantunen

AFFILIATIONS

Microelectronics Research Unit, University of Oulu, P. O. Box 4500, FI-90014, Finland

Note: This paper is part of the APL Special Collection on Advances in 5G Physics, Materials, and Devices.

^{a)} Author to whom correspondence should be addressed: mikko.nelo@oulu.fi

ABSTRACT

A method to realize ultra-low temperature co-fireable ceramic composites with ultra-low permittivity is presented in this work. Hollow glass microspheres with a size of 10–100 μm were used as a filler in a tape based on lithium molybdate (Li_2MoO_4) ceramic to introduce controlled porosity and reduce the relative permittivity of the sintered product. A lamination pressure of only 1.25 MPa was sufficient to produce samples with uniform structure and without delamination. Differential scanning calorimetry and thermogravimetric analysis were used to optimize the sintering temperature profile of the material. The microstructure of the samples was investigated with field emission scanning electron microscopy, and the dielectric properties with a split post dielectric resonator. Compatibility of the composite ceramic with silver was tested by applying thick-film-printed electrodes and post-firing them on the surface. Samples sintered at 540 °C exhibited a relative permittivity of 1.4–5.40 and a loss tangent of 10^{-3} – 10^{-4} at 5 and 10 GHz. The method shows interesting possibilities to significantly reduce processing temperatures compared to conventional low-temperature co-fired ceramics materials and to obtain the extremely low permittivity that is especially required for future high-frequency applications.

Published under license by AIP Publishing. <https://doi.org/10.1063/5.0048566>

The high frequencies used in modern telecommunications such as 5G and beyond will be sensitive to losses in signal pathway due to the absorption by surrounding materials. Furthermore, very low permittivity is also required to enable fast signal propagation and to provide a counter effect for the shrinking size of the components due to the increased frequencies. A common solution to decrease permittivity is to introduce porosity into the materials, which can be done for organic¹ as well as for inorganic² substrates.

Porosity has been added to organic materials, for example, by utilizing foaming agents,³ the partial decomposition of material,⁴ or by utilizing hollow glass microspheres.^{5–7} Hollow glass microspheres (HGMS) offer an inexpensive solution to increase porosity, thereby reducing dielectric permittivity and losses, while better maintaining mechanical rigidity compared to purely gas-filled composites. However, although organic materials offer excellent electrical properties for substrates, their thermal stability can become an issue as power densities of future devices increase.

Ceramic composite materials, on the other hand, offer good thermal stability at higher temperatures. The downside of using ceramic materials has been their high manufacturing temperature, resulting in high energy consumption and increased production costs. Ceramic materials or their glass composites have been developed to be utilized as low-temperature co-fired ceramics (LTCC) sintered typically at

800–1000 °C.^{8,9} For HGMS, these temperatures are still too high (melting temperatures at 700–850 °C), and therefore polymer microspheres or etching has been previously utilized to generate porosity in the ceramic.^{10–13} A low relative permittivity of 3.8 for LTCC has been obtained by Xi *et al.*¹⁴ To further decrease the fabrication temperatures of the ceramics, ultra-low temperature co-fired ceramics (ULTCC) have been developed,^{15–18} which also enable the use of HGMS as presented in this paper.

With the recent invention of a room temperature fabrication method (RTF), a water-based suspension of lithium molybdenum oxide (LMO) has been used to produce bulk dielectric samples and composites.^{19–21} In previous research,² extremely low ϵ_r ceramic-based composite materials were produced at room temperature utilizing water suspension of LMO, HGMS, and quartz fibers. This research showed very good wetting of HGMS with the LMO solution. LMO has been earlier reported²² to have a relatively low sintering temperature of 540 °C with bulk density, relative permittivity, and Qxf of 2.895 g/cm³ (95.5%), 5.5, and 46 000 GHz (13.051 GHz), respectively. In addition, despite the fact that Mo being the transition metal, no extra phases are likely to form as a result of changes in oxidation levels of Mo in such low temperature and ambient sintering atmosphere, which would affect the dielectric properties.^{22–24} This indicates that the combination of LMO and HGMS would also offer an opportunity

to fabricate multilayer structures through ULTCC and tape casting technologies with extremely low ϵ_r and losses for high-frequency applications. In this work, a slurry system for the LMO-HGMS composite for tape casting was further developed from earlier work,²⁵ and the lamination and sintering of several layers was optimized. The high-frequency properties of the composites as a function of HGMS content were studied as well as the achieved microstructures and densities.

The Li_2MoO_4 (LMO) (>99%; Alfa Aesar, USA) powder was milled in ethanol according to the procedure reported earlier by Väättä *et al.*²¹ with ZrO_2 milling media in a planetary ball mill (Pulverisette 6, Fritsch, Idar-Oberstein, Germany) to reduce the particle size and to achieve a suitable size distribution. The dried powder was sieved through a mesh size of 45 μm . The HGMSs (Kevra Oy, Finland) were a C-type glass with 50%–75% of SiO_2 , average sphere size of 40–80 μm , volumetric density of 0.1–0.15 g/cm^3 , bulk density of 0.2 g/cm^3 , and temperature resistance of up to 650 °C according to the datasheet from the manufacturer. According to the SEM-EDS analysis carried out in the earlier work,² the composition of the HGMS was 72 wt. % of SiO_2 , 14 wt. % of Na_2O , and 14 wt. % of CaO . The solvent used in the tape casting slurry was dimethyl carbonate (DMC) (>99%, Sigma-Aldrich, USA), the binder was QPAC® 40–PPC—poly(propylene carbonate) (Empower Materials, Inc, USA), and the plasticizers were Santicizer S160 butyl benzyl phthalate and UCON50HB2000 polyalkylene glycol (Tape Casting Warehouse, Inc, USA).

Tape casting slurries with a designed HGMS content of 0–85 vol. % in the resulting sintered tapes were made. The organic components were first dissolved in DMC, and after the addition of LMO, the solution was milled with zirconium oxide balls for 24 h at a slow speed to thoroughly mix the components and deagglomerate the LMO particles. After milling, the HGMS powder was mixed in with the solution, followed by slow agitation without the milling media to remove the air bubbles from the slurry. The slurries were tape-cast through a 800 μm slit on mylar film and dried under a lid at room temperature to achieve green tapes with a thickness of 200 μm . The compositions of different slurries are shown in Table I.

Decomposition of organic additives and optimization of the sintering profile were studied using DSC-TGA (Netzsch STA 449 F3 Jupiter, NETZSCH-Gerätebau GmbH, Germany). The measurements were carried out in a constant gas flow of 20 ml/min in synthetic air and nitrogen (protective purge) with various temperature profiles. The temperature profile tested with DSC-TGA consisted of five segments: heating to 180 °C (3.6 °C/min), heating to 350 °C (0.7 °C/min), heating to 540 °C (3.2 °C/min), hold at 540 °C (30 min), and cooling to 30 °C (3 °C/min). The sample size in the DCS-TGA measurement varied between 8 and 18 mg.

The green tapes were cut into 40 × 40 mm² squares, and 5–6 layers were stacked and laminated in a uniaxial press with heated plates between silicone sheets to distribute the pressure evenly. The used lamination pressure was 1.25 MPa, temperature 80 °C, and pressing time 15 min. The green density of the laminates was determined through their weight and dimensions. The final sintering profile was as follows: 40 min heating from RT to 140 °C, 10 min hold, 5 h heating to 260 °C, 15 min hold, followed by 1 h heating to 540 °C, 2 h hold. Sintering was finished with 8 h cooling to RT. A long burn out time was used to prevent the formation of gas bubbles in the laminates. A 6.0 g alumina sheet was placed on top of each laminate during the sintering to prevent warping. Weights and dimensions were re-measured after sintering.

Dielectric measurements were carried out with a vector network analyzer (VNA) (Rhodes & Schwarz ZVB20, Germany) connected with a SPDR (QWED, Poland) with nominal resonances at 5.180 and 9.975 GHz. The relative permittivity and dielectric losses were calculated from measurements using the QWED software. After the measurements, conductive silver lines were stencil printed on top of the samples using ESL 599-E (Electro-Science Laboratories, Inc, USA) low temperature silver paste, which was fired at 450 °C following the manufacturer's instructions. Finally, the cross sections of the sintered samples were investigated with field emission scanning electron microscopy (FESEM, Carl Zeiss Ultra Plus, Germany). The samples for FESEM analysis were laser-cut and finished with ion polishing (Jeol IB-19520CCP, Jeol Ltd., Japan).

The decomposition of the organic additives in the DSC measurement is shown in Fig. 1. The onset of the first exothermic peak in the DSC data started around 150 °C, and between 150 and 180 °C, the organics started to burn out from the green tape, which was also detected as a small decline in the TG curve due to mass loss. The largest mass loss and sharp exothermic peaks were seen around 190–200 °C. The heating was considerably slowed in this region to prevent the formation of gas bubbles in the final product. After about 250 °C, the organic additives had decomposed and no further mass loss or reactions were detected. These results are well in line with measurements reported earlier.²⁵

According to the FESEM analysis, no delamination of the layers was observed and the silver ink was attaching sufficiently well to the sample surfaces up to 50 vol. % HGMS content. With higher HGMS content, the mechanical integrity of the sintered samples started to decline. The cross sections are presented in Fig. 2.

The measured dielectric properties, the shrinkages, and densities of the tapes are presented in Table II. It can be seen that with increasing HGMS content, the relative permittivity greatly and continuously decreased at both frequencies, while the loss tangent values had the

TABLE I. Composition of the tape casting slurries.

Vol. % of HGMS in sintered tape	HGMS (g)	LMO (g)	QPAC 40 (g)	Santicizer S160 (g)	Polyalkylene glycol (g)	DMC (g)
0 % HGMS	0	28	3.6	0.9	0.9	28
25 % HGMS	0.5	21	3.1	0.75	0.75	28
50 % HGMS	1.0	14	3.3	0.8	0.8	28
75 % HGMS	1.5	7.0	3.5	0.9	0.9	28
85 % HGMS	1.7	4.2	3.6	0.9	0.9	28

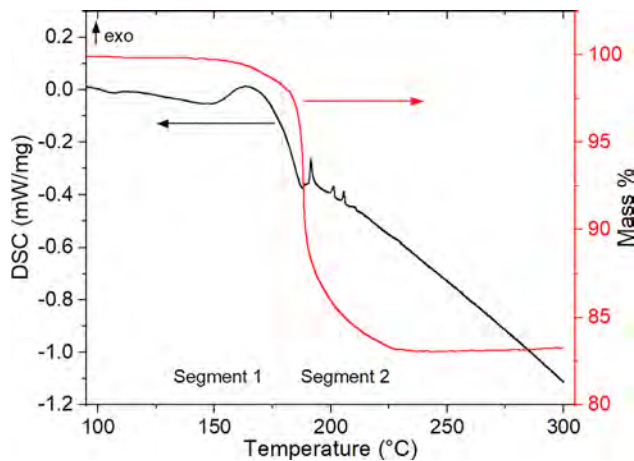


FIG. 1. DSC-TGA measurement of a green tape containing 50 vol. % of HGMS. The two heating segments with weight loss occurring are presented. The organic materials decomposed at 150–225 °C.

opposite behavior. Supposedly, the level of losses could be hindered by the selection of a different type of HGMS. The shrinkage of the samples also reduced when the HGMS content was increased as a consequence of the reduced amount of LMO that sinters. The samples were easy to handle until 75 and 85 vol. % HGMS content, which were rather brittle samples and needed extra care in handling.

The conclusion of the materials' properties is shown in Table III along with some other low permittivity materials. The permittivity of the 50 vol. % was less than half that of the sintered LMO (5.4). When comparing dielectric properties with other low permittivity microwave materials in the table, the developed composites with 50 vol. % or more HGMS had the lowest permittivities and still lower loss tangents than all other composites. Polymer—ceramic_{A6M}¹⁰ being the only one with a comparable loss tangent, but with a permittivity 44% higher. Also, the sintering temperature remained the lowest of these materials if the polymer composites and RTF are not considered. This shows the high potential of the developed composite for ULTCC application specific optimization, by tuning the filler content (e.g., 50–85 vol. %) according to the wanted high frequency, (low) permittivity, and the tolerable losses.

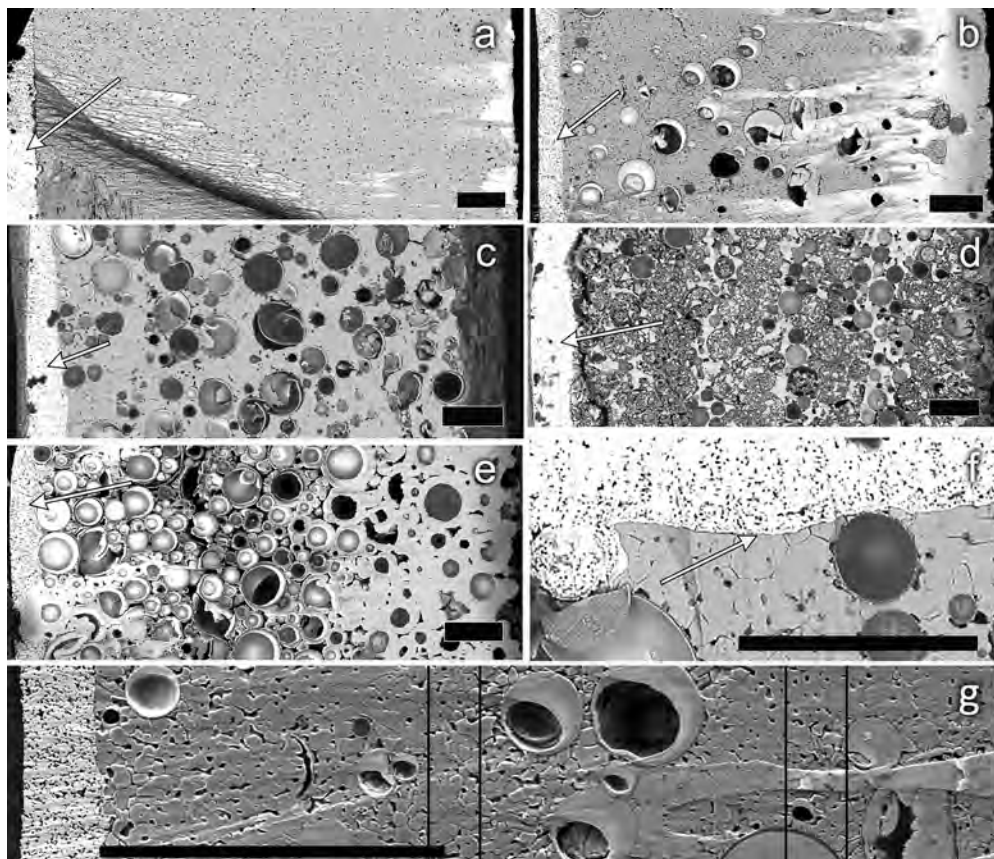


FIG. 2. Backscattering images of cross sections of sintered samples. Silver layer can be seen as a brighter layer on the left side of each sample, indicated with an arrow. (a) Pure LMO, (b) 25 vol. % HGMS, (c) 50 vol. % HGMS, (d) 75 vol. % HGMS, and (e) 85 vol. % HGMS. (f) Printed silver ink interface with sample containing 50 vol. % HGMS. (g) Magnification of 25 vol. % HGMS sample with three 200 μm thick layers in the image area. Vertical lines indicate the location of estimated layer surfaces, as they were not visible in FESEM inspection. Scale bars on figures (a)–(f) 100 μm and (g) 200 μm.

TABLE II. Properties of tapes.

Tape contents	5.2 GHz		10 GHz		Density g/cm ³	Density % of LMO	Shrinkage	
	ϵ_r	$\tan \delta$, E-3	ϵ_r	$\tan \delta$, E-3			XY, %	Z, %
0 % HGMS	5.4	0.17	5.4	0.19	2.84	93 %	21 %	21 %
25 % HGMS	3.5	0.60	3.5	0.65	1.77	58 %	13 %	14 %
50 % HGMS	2.6	1.1	2.6	1.3	1.32	43 %	8 %	8 %
75 % HGMS	1.7	1.2	1.7	1.3	0.62	20 %	4 %	3 %
85 % HGMS	1.4	1.4	1.5	1.7	0.39	13 %	4 %	-4 %

A simple method to produce low permittivity and low dielectric loss LMO-based ceramic suitable for ULTCC and sinterable at 540 °C was developed. DSC-TG analysis was utilized to optimize the sintering profile for the tape material especially in the case of high HGMS content (50 vol. % or more). Careful development of manufacturing parameters resulted in green tapes with easy handling and lamination characteristics, with an exceptionally low lamination pressure of 1.25 MPa. The low lamination pressure may enable the embedding of delicate discrete components inside the laminated structures, which opens up new possibilities for future research. The used silver paste seemed to be suitable for use with the developed LMO-based composition, thus the developed material may be used in ULTCC as expected. The HGMS filler reduced the density of the ULTCC to 13% (85 vol. % HGMS) of the pure ULTCC LMO (0 vol. % HGMS), and it also greatly affected the dielectric properties. The lowest achieved relative permittivity

was 1.4 and 1.5 at 5.2 and 10 GHz, respectively, for the sample containing 85 vol. % HGMS. The lowest loss tangent values achieved were 1.7 and 1.9×10^{-4} at 5.2 and 10 GHz, respectively, for the sample containing 0 vol. % HGMS (or sintered LMO) and increased to 1.4 and 1.7×10^{-3} , respectively, with the 85 vol. % HGMS. The developed material system showed one of the lowest permittivities and losses among a large variety of microwave ceramic and composite materials reported. The dielectric permittivity and losses of the developed materials could be easily adjusted by using different quantities of HGMS.

M.N. produced and measured all samples and obtained the used materials. T.V. formulated the tape casting slurries and produced the green tapes used in this work. T.S. carried out the DSC-TG analysis of the green tape. H.J. and J.J. formulated the hypotheses and discussed the dielectric results of the study. All authors contributed to the writing of the manuscript and evaluation of the results.

TABLE III. Microwave properties of low permittivity materials.

Material type	Filler	Load (%)	Fabr. Temp. (°C)	Meas. freq. (GHz)	ϵ_r	Loss tan, E-3	Qxf, E9	Density (g/cm ³)	Ref.
ceramic	Li ₂ MoO ₄	100	540	5.2–10	5.4	0.17–0.19	...	2.84 (93%)	this study
glass—ceramic	HGMS	85–25 vol.	540	5.2–10	1.4–3.5	1.7–0.6	...	0.39–1.77 (13–58%)	this study
Glass - polymer	glass balls	46.7–18.5 vol.	140	0.01	2.59–3.0	1.29–1.64	...	0.930–1.1 (73–90%)	7
Commercial LTCC	10	4.2–19	6–6.6	360–10 000	...	8
Commercial LTCC	10	4.7–19	1–6	1667–10 000	...	8
Polymer—ceramic _{A6M}	PMMA spheres	30 wt.	500	5–10	3.75	0.85–1.25	...	1.55 (67%)	10
Polymer—ceramic ₉₅₁	PMMA spheres	30 wt.	500	5–10	6.5–6.5	5.8–6.7	...	2.91 (98%)	10
Glass-Al ₂ O ₃	graphite	50 wt.	1250	0.002	2.8	11
Glass-cordierite	Graphite	25 wt	1250	0.002	3.7	11
Ceramic—glass	Al ₂ O ₃	10–15 wt	640	16.64	3.9–3.5	...	38 000–12 500	2.87–2.75	14
Ceramic	Li ₂ MoO ₄	100	25–120	9.60	4.6–5.2	...	10 200–18 500	2.6–2.8 (87–93%)	19
Glass—ceramic, LTCC	Silica	15 wt	650	0.001	6.4	1.00	...	3.6	26
ceramic	K ₂ Mo ₃ O ₁₀	100	520	...	5.6	...	35 830	...	27
Glass—ceramic	Glass	50 vol.	750–950	12.4–12.6	6.6–5.8	...	2632	2.8–3.0	28
ceramic	Na ₂ O–MoO ₃	100	660	13.39	4.1	...	35 000	2.98 (92%)	29

The work leading to these results received funding from the European Research Council (ERC) under the ERC POC Grant Agreement No. 812837. This work was supported in part by the Academy of Finland 6Genesis Flagship (Grant No. 318927), Printed Intelligence Infrastructure (PII) (Grant No. 320017), and in part by the European Regional Development Fund project 'Novel digitally fabricated materials for electronics, optics and medical applications (NOVIDAM)', Grant No. A74080.

DATA AVAILABILITY

The data that support the findings of this study are available from the corresponding author upon reasonable request.

REFERENCES

- G. F. Zhao, T. Ishizaka, H. Kasai, M. Hasegawa, T. Furukawa, H. Nakanishi, and H. Oikawa, "Ultralow-dielectric-constant films prepared from hollow polyimide nanoparticles possessing controllable core sizes," *Chem. Mater.* **21**, 419 (2009).
- M. Nelo, H. Liimatainen, M. Väättäjä, J. Ukkola, J. Juuti, and H. Jantunen, "Solid air-Low temperature manufacturing of ultra-low permittivity composite materials for future telecommunication systems," *Front. Mater.* **6**, 94 (2019).
- B. Zhao, C. Zhao, C. Wang, and C. B. Park, "Poly(vinylidene fluoride) foams: A promising low-k dielectric and heat-insulating material," *J. Mater. Chem. C* **6**, 3065–3073 (2018).
- W. C. Wang, R. H. Vora, E. T. Kang, K. G. Neoh, C. K. Ong, and L. F. Chen, "Nanoporous ultra-low-k films prepared from fluorinated polyimide with grafted poly(acrylic acid) side chains," *Adv. Mater.* **16**, 54 (2004).
- L. N. Chellis, R. M. Japp, W. J. Summa, W. J. Rudik, and D. W. Wang, "Flame retardant, low dielectric constant microsphere filled laminate," Patent US5126192A.
- D. Kellerman, "Micro-electronics devices and methods of manufacturing same," Patent US4781968A.
- J. Chen, D. Meng, Y. Feng, N. Li, A. Krivda, F. Greuter, and J. Rocks, "Epoxy composites with glass bubbles for electrical application," in *Electrical Insulation Conference* (2013), pp. 20–24.
- M. T. Sebastian and H. Jantunen, "Low loss dielectric materials for LTCC applications: A review," *Int. Mater. Rev.* **53**, 57–90 (2008).
- J. Zhou, "Towards rational design of low-temperature co-fired ceramic (LTCC) materials," *J. Adv. Ceram.* **1**, 89–99 (2012).
- M. Sobocinski, M. Teirikangas, J. Peräntie, T. Vahera, M. Nelo, J. Juuti, and H. Jantunen, "Decreasing the relative permittivity of LTCC by porosification with poly(methyl methacrylate) microspheres," *Ceram. Int.* **41**, 10871–10877 (2015).
- B. Synkiewicz, D. Szwagierczak, and J. Kulawik, "Multilayer LTCC structures based on glass-cordierite layers with different porosity," *Microelectron. Int.* **34**, 110–115 (2017).
- A. Bittner and U. Schmid, "Permittivity of LTCC substrates porosified with a wet chemical etching process," *Procedia Eng.* **5**, 327–330 (2010).
- R. K. Nishihara, P. L. Rachadel, M. G. Novy, and Q. D. Hotza, "Manufacturing porous ceramic materials by tape casting—A review," *J. Eur. Ceram. Soc.* **38**, 988–1001 (2018).
- J. Xi, G. Chen, F. Liu, F. Shang, J. Xu, C. Zhou, and C. Yuan, "Synthesis, microstructure and characterization of ultra-low permittivity CuO–ZnO–B₂O₃–Li₂O glass/Al₂O₃ composites for ULTCC application," *Ceram. Int.* **45**, 24431–24436 (2019).
- M. T. Sebastian, H. Wang, and H. Jantunen, "Low temperature co-fired ceramics with ultra-low sintering temperature: A review," *Curr. Opin. Solid State Mater. Sci.* **20**, 151–170 (2016).
- J. Varghese, T. Siponkoski, M. Sobocinski, T. Vahera, and H. Jantunen, "Multilayer functional tapes cofired at 450°C: Beyond HTCC and LTCC technologies," *ACS Appl. Mater. Interfaces* **10**, 11048–11055 (2018).
- S.-Z. Hao, D. Zhou, F. Hussain, W.-F. Liu, J.-Z. Su, D.-W. Wang, Q.-P. Wang, Z.-M. Qi, C. Singh, and S. Trukhanov, "Structure, spectral analysis and microwave dielectric properties of novel $x(\text{NaBi})_{0.5}\text{MoO}_4\text{-(1-x)Bi}_{2/3}\text{MoO}_4$ ($x=0.2\sim0.8$) ceramics with low sintering temperatures," *J. Eur. Ceram. Soc.* **40**, 3569–3576 (2020).
- H.-H. Guo, D. Zhou, C. Du, P.-J. Wang, W.-F. Liu, L.-X. Pang, Q.-P. Wang, J.-Z. Su, C. Singh, and S. Trukhanov, "Temperature stable $\text{Li}_2\text{Ti}_{0.75}\text{Nb}_{2/3}\text{O}_{0.25}\text{O}_3$ -based microwave dielectric ceramics with low sintering temperature and ultra-low dielectric loss for dielectric resonator antenna applications," *J. Mater. Chem. C* **8**, 4690–4700 (2020).
- H. Kähäri, M. Teirikangas, J. Juuti, and H. Jantunen, "Dielectric properties of lithium molybdate ceramic fabricated at room temperature," *J. Am. Ceram. Soc.* **97**, 3378–3379 (2014).
- H. Kähäri, M. Teirikangas, J. Juuti, and H. Jantunen, "Improvements and modifications to room-temperature fabrication method for dielectric Li_2MoO_4 Ceramics," *J. Am. Ceram. Soc.* **98**, 687–689 (2015).
- M. Väättäjä, H. Kähäri, J. Juuti, and H. Jantunen, " Li_2MoO_4 -based composite ceramics fabricated from temperature- and atmosphere-sensitive MnZn ferrite at room temperature," *J. Am. Ceram. Soc.* **100**, 3626–3635 (2017).
- D. Zhou, C. A. Randall, H. Wang, L. X. Pang, and X. Yao, "Microwave dielectric ceramics in $\text{Li}_2\text{O-Bi}_2\text{O}_3\text{-MoO}_3$ system with ultra-low sintering temperatures," *J. Am. Ceram. Soc.* **93**, 1096–1100 (2010).
- S. Kumakura, Y. Shirao, K. Kubota, and S. Komaba, "Preparation and electrochemical properties of $\text{Li}_2\text{MoO}_3/\text{C}$ composites for rechargeable Li-ion batteries," *Phys. Chem. Chem. Phys.* **18**, 28556–28563 (2016).
- I. Z. Zhumatayeva, I. E. Kenzhina, A. L. Kozlovskiy, and M. V. Zdorovets, "The study of the prospects for the use of $\text{Li}_{0.15}\text{Sr}_{0.85}\text{TiO}_3$ ceramics," *J. Mater. Sci.* **31**, 6764–6772 (2020).
- N. Joseph, J. Varghese, M. Teirikangas, T. Vahera, and H. Jantunen, "Ultra-low-temperature cofired ceramic substrates with low residual carbon for next-generation microwave applications," *ACS Appl. Mater. Interfaces* **11**, 23798–23807 (2019).
- H. Yu, K. Ju, J. Liu, and Y. Li, "Tape casting and dielectric properties of SiO_2 -filled glass composite ceramic with an ultra-low sintering temperature," *J. Mater. Sci.* **25**, 5114–5118 (2014).
- Gq Zhang, J. Guo, L. He, D. Zhou, H. Wang, J. Koruza, and M. Kosec, "Preparation and microwave dielectric properties of ultra-low temperature sintering ceramics in $\text{K}_2\text{O-MoO}_3$ Binary System," *J. Am. Ceram. Soc.* **97**, 241–245 (2014).
- S.-O. Yoon, S.-H. Shim, K.-S. Kim, J.-G. Park, and S. Kim, "Low-temperature preparation and microwave dielectric properties of ZBS glass– Al_2O_3 composites," *Ceram. Int.* **35**, 1271–1275 (2009).
- Gq Zhang, H. Wang, J. Guo, L. He, Dd Wei, and Qb Yuan, "Ultra-low sintering temperature microwave dielectric ceramics based on $\text{Na}_2\text{O-MoO}_3$ Binary System," *J. Am. Ceram. Soc.* **98**, 528–533 (2015).